ELSEVIER

Polymer 41 (2000) 101–109

polymer

Solid state NMR studies of hydrogen bonding network formation of novolac type phenolic resin and poly(ethylene oxide) blend

P.P. Chu*, H.-D. Wu

Department of Chemistry, National Central University, Chung-Li 32054, Taiwan

Received 2 June 1998; received in revised form 30 September 1998; accepted 28 January 1999

Abstract

Solid state NMR studies revealed the hydrogen bonding network characteristics and the substantial changes of molecular motion in phenolic/PEO blend. The PEO crystallinity was reduced owing to the formation of strong hydrogen bonding between PEO and phenolic, as revealed by ^{13}C chemical shift and DSC. Both $T_{1\rho}^{H}$ relaxation behavior at high field and T_1^H relaxation time distribution taken at low field reflected the substantial increase of molecular segmental mobility upon blending. The maximum flexibility appeared at 40/60 (phenolic/PEO) composition is attributed to the balance between the amount of amorphous PEO and the effective pairing of hydrogen bonding between the two components. The seemingly contradicting results between the increase of overall motion with the free volume contraction and glass temperature elevation has raised the point that these measurements are ensemble averages of different length scales. Correlation between properties and motion revealed by spin relaxation should proceed with caution.

Keywords: Novolac; Phenolic/PEO blend; NMR spectra

1. Introduction

Phenolic resin is widely used in industries for the manufacture of paints, adhesives, and composites, owing to its low cost, dimension stability, and fire-proofing capability [1]. The brittle nature however, has significantly limited its usage. Many efforts are being delved to improve the structural and decorative properties through blending [2–4]. As illustrated previously [5,6–10], the hydroxyl group in phenolic provides the hydrogen donor forming hydrogen bonding with polymers containing hydroxyl, carbonyl, ether or other proton-accepting segments. Several such polymers have been successfully used as modifies to tailor the phenolic physical properties [4,5,6,7] and this inter-polymer association has been identified as the major driving force for miscibility between phenolic and the modifiers.

A less addressed issue beyond miscibility, however, is that molecular segmental motion can also be modulated due to the modifier motional characteristics. The change of molecular motion is especially pronounced in the case of phenolic/PEO blend, where there is unusual increase of molecular motion in spite of the clear evidence that strong hydrogen bonding appears [11,12]. To this end, we have employed several solid state NMR techniques, such as ^{13}C CP/MAS; chemical shift; proton spin–lattice relaxation time in the rotating frame ($T_{1\rho}^{H}$); and the low magnetic field proton relaxation time (T_1^H) to explore the inter-molecular hydrogen bonding structures and the molecular motion of the phenolic/PEO blends. Combined with the understanding of the crystallinity from DSC results, factors influencing molecular motion can be fully illustrated. This also raised the issue that molecular motion measured from spin relaxation and thermodynamics parameters such as free volume and T_g are ensemble averages of different length scale.

2. Experimental section

2.1. Sample preparation

The novolac type phenolic resin was synthesized and analyzed as described previously [13]. The chemical structure of the novolac type phenolic resin consists of phenol rings bridge-linked randomly by methylene groups with 19% ortho–ortho, 57% ortho–para, and 24% para–para methylene bridges as identified by the solution ^{13}C NMR. The phenolic resin does not contain any reactive phenol group that can cause cross-linking on heating. The poly(ethylene oxide) (PEO) was obtained from (Union Carbide

* Corresponding author. Tel.: + 886-3-425-8631; fax: + 886-3-422-7664.

E-mail address: pjchu@rs970.ncu.edu.tw (P.P. Chu)

0032-3861/00/$ - see front matter
PII: S0032-3861(99)00098-1

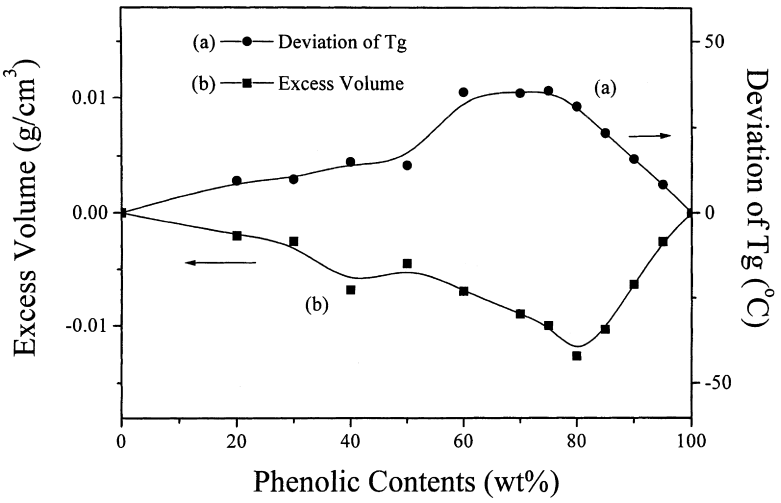

Fig. 1. The composition dependent T_g deviation and excess volume of phenolic/PEO blend. (a) T_g deviation; (b) excess volume.

Co. USA, $M_n = 200\,000$). The phenolic/PEO blends were prepared by mixing the desired compositions in THF (1% (w/v)) solution at room temperature. The mixture was stirred for 6–8 h, and allowed to evaporate slowly at room temperature under vacuum for one day, and then dried at 50°C for additional two days followed by annealing at 140°C for 2 h under vacuum. The cross-linked novolac type phenolic resin and various phenolic/PEO blends were achieved with 10 wt.% hexamine (based to phenolic) cross-linking agent. Hexamine containing solution was completely mixed by stirring and dried at 50°C for two days in an oven, and cured at 160°C for 2 h in vacuum. The residual THF is completely removed based upon the solid state NMR results.

2.2. Characterization

The glass transition temperatures (T_g) of the polymer blend films were determined by differential scanning calorimeter (Du-Pont, DSC Model 2900). The scan rate was 20°C/min ranging from −80 to 100°C. The measurements were made with 3–4 mg of samples on DSC plate using the second scan after the specimens were quickly cooled to room temperature following the first heating. The T_g value was determined from the midpoint of the transition point of the heat capacity change with a reproducibility estimated to be within ±2°C. Specific volumes were determined at 25°C using a dilatometer calibrated with *n*-heptane. The temperature of the water bath was maintained constant to within 0.1°C. From repeated measurements, the volume has a standard deviation of ±0.001 cm^3/g.

High resolution solid state ^{13}C NMR experiments were carried out on a Bruker DSX-300 spectrometer operating at resonance frequencies of 300.13 and 75.475 MHz for ^1H and ^{13}C, respectively. The ^{13}C CP/MAS spectra were measured with a 3.9 μs 90° pulse; 3 s pulse delay time; 30 ms acquisition time; and 2048 number of scans. All NMR spectra were taken at 300 K with broad band proton decoupling and normal cross-polarization pulse sequence. 5.4 kHz magic angle sample spinning (MAS) rate was used to avoid overlapping absorption. The chemical shifts of ^{13}C spectra were secondary referenced to the carbonyl of Glycine at 176.04 ppm (referenced to TMS). The proton spin–lattice relaxation time in the rotating frame ($T^H_{1\rho}$) was measured indirectly via carbon observation using a 90°-τ-spin lock pulse sequence prior to cross-polarization. The data acquisition was performed via ^1H decoupling, and delay time (τ) ranging from 0.1 to 16 ms with contact time of 1.0 ms.

The proton spin–lattice relaxation time (T^H_1) measurements in low magnetic field were carried out on a Bruker NMS-20 Minispec system with proton resonance frequency of 20 MHz, performed at 40°C. T^H_1 was measured using inversion recovery pulse sequence using 1 μs 90°C pulse and 1 μs dead time. The hard pulse and short dead time allow for the detection of the very short T_2 components, even without the use of a refocusing sequence. Typically, the T^H_1 was measured with 32 number of scans and 3 s recycle delay. Numerical procedures in constructing the relaxation time distribution are described elsewhere [14,15].

3. Results and discussion

3.1. Deviation of T_g and excess volume of phenolic/PEO blend

Thermal properties of the phenolic/PEO blend has been clearly studied previously [16]. The phenolic resin is completely amorphous and is known to be rigid with concentrated hydrogen bonding association, while PEO resin shows high crystalline with weak inter-molecular interaction. Prior results confirm that the inter-molecular hydrogen bonding between blend components has driven

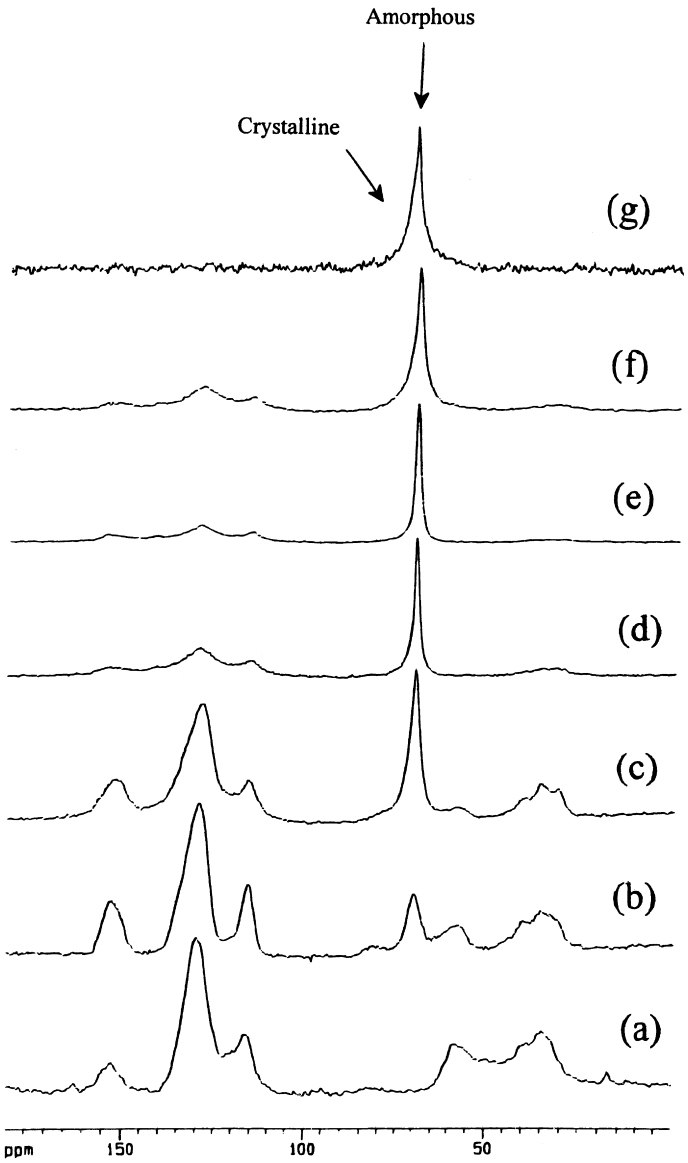

Fig. 2. The typical ^{13}C CP/MAS spectra of PEO, and uncured phenolic/PEO blends measured by the normal CP/MAS method. (a) 100/0; (b) 80/20; (c) 60/40; (d) 50/50; (e) 40/60; (f) 30/70; (g) 0/100 phenolic/PEO blends.

the miscibility between the two components, in spite of their large structural differences [6,9,10]. Single T_g observed for all the blend composition confirms that these blends are highly miscible on the basis of thermodynamics.

The deviation of T_g from linearity is obtained following the Fox [17] relationship:

$$\Delta T_g = T_g - \frac{1}{\omega_a/T_{gb}^0 + \omega_b/T_{gb}^0}, \quad (1)$$

where ω_i is the weight fraction of component i, and T_{gi}^0 is the glass transition temperature of the corresponding pure component, while T_g is the measured value for the blend. Excess volume monitors the effect of interactions and conformations of the mixtures [18,19] and contrast with the T_g results. In the presence of the hydrogen bonding, free volume may deviate from additive relationship. The excess free volume (V^E) is defined as:

$$V^E = V - (\omega_a V_a^0 + \omega_b V_b^0), \quad (2)$$

where ω_i is the weight fraction of component i, and V_i^0 is the specific volume of the pure component, i. V is the experimentally measured specific volume of the phenolic/PEO blend.

Fig. 1 illustrates the composition dependent T_g deviation and excess volume of phenolic/PEO blends. The T_g deviation is positive and the excess free volume is negative throughout the blend compositions, with the most pronounced deviations appearing in the phenolic rich region. A maximum T_g of 35°C appeared at 75/25 phenolic/PEO composition and negative excess volume gives two

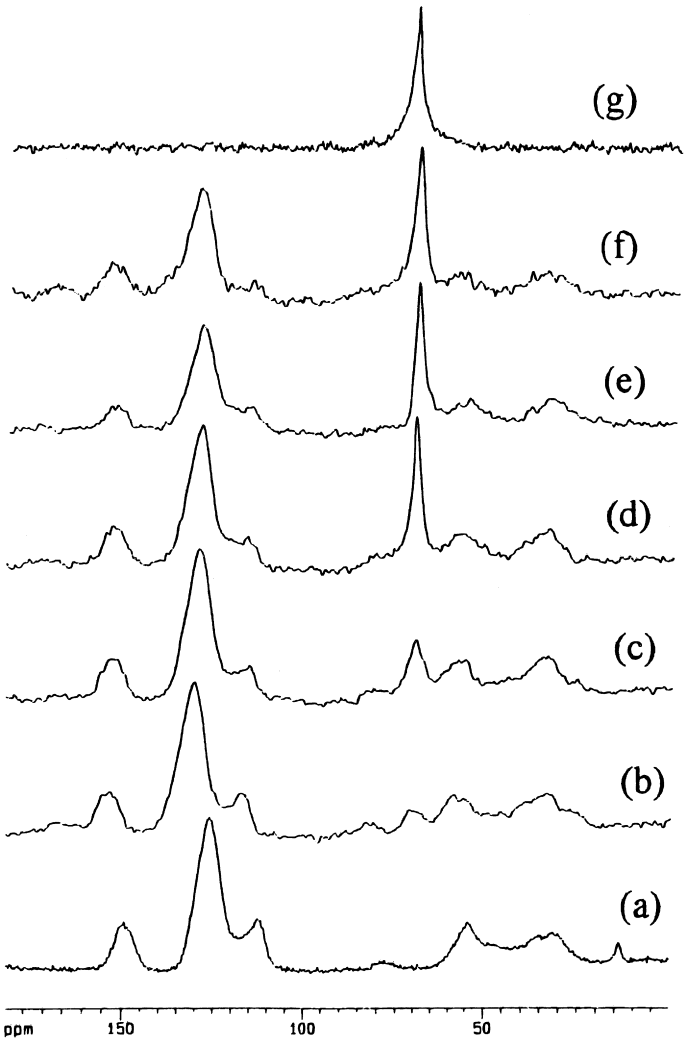

Fig. 3. The typical ^{13}C CP/MAS spectra of PEO, and cured phenolic/PEO blends measured by the normal CP/MAS method. (a) 100/0; (b) 80/20; (c) 60/40; (d) 50/50; (e) 40/60; (f) 30/70; (g) 0/100 phenolic/PEO blends.

minima occurred at the neighborhood of 80/20 and 40/60 phenolic/PEO compositions are observed. The positive T_g and negative excess volume deviations are consistent with conventional theory for the glass transition temperature which shows that T_g is inversely related to free volume. Both T_g and free volume results give direct support that the concentrated hydrogen bonding has lead to a much compacted blend structure with lower entropy. One would then expect the phenolic/PEO blend to exhibit more restricted segmental motion due to the lower entropy and smaller free volume. However, substantial increase of the molecular motion is detected, instead. The anomaly can be examined from the change of hydrogen bonding configuration and the change of PEO crystallinity upon blending using the solid state NMR.

Table 1
The chemical shifts of phenolic and PEO in NMR spectrum

Components	Chemical shift (ppm)	Description
Phenolic	32	Methylene
	114	Ortho-substituted in phenol ring
	152	Hydroxyl-substituted in phenol ring
	126	Other carbon in phenol ring
PEO	72	Crystalline PEO
	70	Amorphous PEO

3.2. ^{13}C chemical shifts of NMR spectra

The PEO crystallite shows a monoclinic crystal structure with a seven-residue/two-turn helix conformation [20,21]. The crystalline and the amorphous PEO can be clearly identified through the solid state ^{13}C NMR chemical shifts [22]. Previously, Zhang et al. had observed a narrow (ca. 70 ppm) and broad components (ca. 72 ppm) in ^{13}C resonance for methylene carbons in PEO with varying temperatures [23]. Typical ^{13}C CP/MAS NMR spectra of the phenolic/

Table 2
The chemical shifts and peak width of hydroxyl-substituted carbon in phenolic and amorphous PEO for cured and uncured various blend compositions (contact time of 1 ms)

Samples		Hydroxyl-substituted carbon in phenolic		Methylene of PEO (Amorphous)	
		Chemical shift (ppm)	Peak width (Hz)	Chemical shift (ppm)	Peak width (Hz)
Uncured phenolic/PEO ratio					
(a)	100/0	151.2	488		
(b)	80/20	151.2	492	69.89	371
(c)	60/40	150.9	550	69.94	297
(d)	50/50	152.1	667	69.83	239
(e)	40/60	153.3	723	69.89	194
(f)	30/70	153.5		69.91	447
(g)	0/100			72.2[a]	1019[a]
Cured phenolic/PEO ratio					
(a)	100/0	151.3	483		
(b)	80/20	151.4	485	70.1	469
(c)	60/40	151.7	517	70.1	364
(d)	50/50	151.9	525	70.3	275
(e)	40/60	152.3	575	70.0	235
(f)	30/70			70.5	510

[a] Crystalline state.

PEO blends are shown in Fig. 2 for the uncured and in Fig. 3 for the cured samples with shift assignments summarized in Table 1. The contact time longer than 1 ms results in substantial suppression for the phenolic carbons, making it hard to study ^{13}C signal for other molecular segments. In order to observe both the amorphous and the crystalline PEO, which requires large time scale difference to optimize cross-polarization, an intermediate contact time of 1 ms is used. For better comparison, the chemical shift and the peak width of the hydroxyl-substituted (α) carbon in the phenolic and the methylene carbon in the PEO for cured and uncured

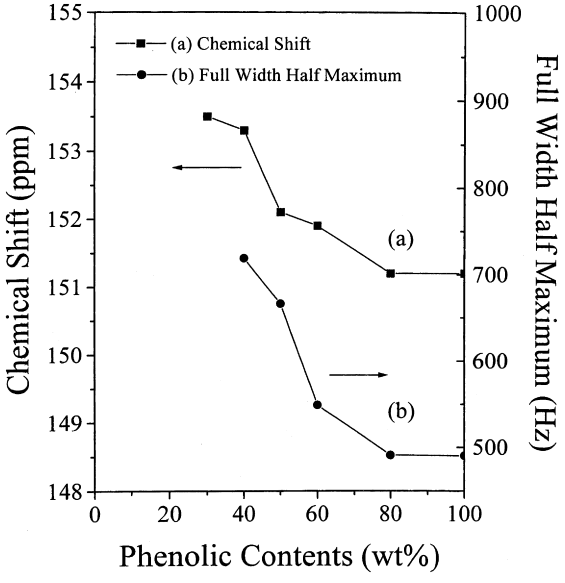

Fig. 4. The chemical shift and full width half maximum of hydroxyl group of various uncured phenolic/PEO blend compositions. (a) chemical shift (■); (b) full width half maximum (●).

blends are summarized in Table 2. As clearly seen in Fig. 2(g) (pure PEO), a sharp resonance corresponds to highly mobile amorphous PEO centered at 70 ppm is superimposed with a broad resonance corresponds to crystalline PEO centered at 72 ppm. With increasing phenolic content, the crystalline component disappeared and gradually replaced with the 70 ppm species. The narrowest PEO resonance occurred at 40/60 (phenolic/PEO) composition, which reflected the dramatic changes in mobility to be discussed in the following section. Similar trends are also reproduced in Fig. 3 for the cured blends. When phenolic becomes the major component, the peak broadens again. This is either due to the chemical shift distribution in the amorphous phenolic/PEO moiety or the coincidence of motional frequency with the proton decoupling frequency (~60 kHz).

Hydrogen bonding formation can be clearly observed from α carbon chemical shift of the phenolic. Previous study revealed that the carbon next to the hydrogen bonded moiety is down-field shifted (de-shielding) with respect to the one without hydrogen bonding [5]. As shown in Fig. 4, the α carbon resonance in the pure uncured phenolic appeared at 151.2 ppm. With increasing PEO content, the resonance shifted continuously down-field revealed the gradual increase in hydrogen bonding. A similar trend is repeated in the cured phenolic/PEO blends. Owing to the fact that ether carbon is less sensitive to the hydrogen bonding, shift in amorphous PEO methylene resonance is not as pronounced as that from the carbonyl.

Curing has changed molecular motion. This is evident from the difference of peak intensities in the aromatic resonance (Fig. 3). The stronger phenolic resonance in the cured sample reflects the higher cross polarization efficiency. It is

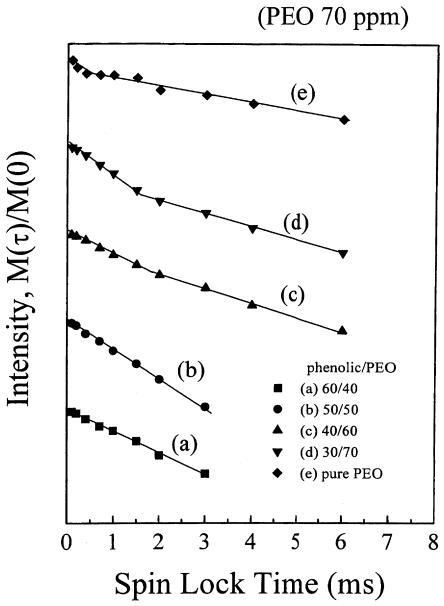

Fig. 5. The semi-logarithmic plots of the magnetization intensities of PEO versus the spin-lock time for uncured phenolic/PEO blends at contact time of 1 ms. (a) 60/40 (■); (b) 50/50 (●); (c) 40/60 (▲); (d) 30/70 (▼); and (e) 0/100 (◆), phenolic/PEO blends.

possible that, curing has initiated cross-linking which hinders the molecular motion of the blend matrix and improves the cross-polarization efficiency.

Although, ^{13}C spectra hinted the interplay of crystalline PEO and molecular motion, detail studies of segmental mobility upon blending can be most effectively derived from $T_{1\rho}^H$ and T_1^H studies. Both $T_{1\rho}^H$ and T_1^H are powerful measures to the compositional heterogeneity and the

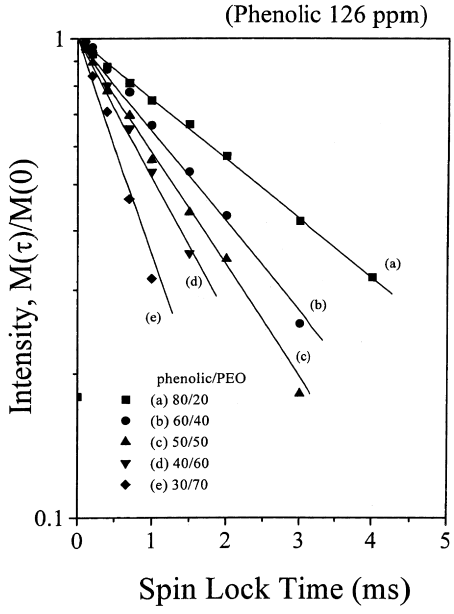

Fig. 6. The semi-logarithmic plots of the magnetization intensities of 126 ppm (benzene ring of phenolic) versus the spin-lock time for cured phenolic/PEO blends at contact time of 1 ms. (a) 80/20 (■); (b) 60/40 (●); (c) 50/50 (▲); (d) 40/60 (▼); (e) 30/70 (◆), phenolic/PEO blends.

molecular segmental motion in length scales limited by spin diffusion. The main difference between the $T_{1\rho}^H$ and the T_1^H is that they responded to different time scale. The T_1^H with a longer time scale (100 ms to few seconds) is the ensemble average of motion over larger length scale within few hundred Å, while $T_{1\rho}^H$ with a shorter time scale (few milliseconds), is the average of the motion within shorter length scale of ~50 Å, based upon a crude estimation using proton–proton spin diffusion constant of 10^{-12} cm^2/s. The two properties would provide different aspects of the segmental motion, suitable for the study of polymer blend.

3.3. $T_{1\rho}^H$ relaxation time

The $T_{1\rho}^H$ relaxation behaviors of the blends are shown in Fig. 5 (PEO, 70 ppm) and Fig. 6 (phenolic, 126 ppm), respectively. The $T_{1\rho}^H$ values derived from the binary exponential analysis are tabulated for both the cured and the uncured samples in Table 3. Regression statistics shows that the relaxation time measurements has a standard error of ±0.5 ms.

As shown in Fig. 5, single exponential decay is observed with high phenolic content, but gradually shows bi-exponential decay at higher PEO content. The short and long relaxation components of PEO are attributed to the amorphous and crystalline phases for PEO respectively, based upon previous study [23]. As seen in Table 3, the amorphous $T_{1\rho}^H$ decreases with increasing PEO, and bifurcated as the PEO content grows above 70 wt.%. In phenolic rich region, increases in $T_{1\rho}^H$ (amorphous) suggests that the polymer motion is reduced, which reflects the more rigid character of the phenolic. In the PEO rich region, a decrease of the $T_{1\rho}^H$ value is associated with the increase of mobility in amorphous PEO which is related to the reduction of inter-molecular hydrogen bonding strength. Increasing amount of the long component with increasing PEO content suggests that more crystalline PEO appeared.

The relaxation for phenolic is depicted in Fig. 6. As seen from Table 3, phenolic exhibits only single relaxation throughout all blends, indicating good miscibility and dynamic homogeneity in the phenolic domain. Interestingly, the $T_{1\rho}^H$ (phenolic) decreases continuously with increasing PEO which approaches that of pure PEO in the neighborhood of 40/60 composition. The result affirms that the overall miscibility was established at this composition. Prior calorimetric study shows that the crystalline PEO is completely destroyed when phenolic increases beyond 40 wt.%. In addition, all $T_{1\rho}^H s$ (phenolic) in the blends are shorter than the parent phenolic and hinted that phenolic mobility also increases continuously with increasing PEO.

Both ^{13}C chemical shift and $T_{1\rho}^H$ support that the hydrogen bonding within phenolic gradually shifted to PEO through inter-polymer association. The strong association has motivated intimate miscibility between the phenolic and the PEO, making up the amorphous domain and raised the mobility of the phenolic moiety. It is also clear that the

Table 3
The $T_{1\rho}^{H}$ value of the uncured and the cured various phenolic/PEO blends composition. (The contact time is 1 ms)

		126 ppm		70 ppm	
Uncured phenolic/PEO ratio					
(a)	100/0	3.24			
(b)	80/20	2.25			
(c)	60/40	2.08		2.21	
(d)	50/50	1.22		1.26	
(e)	40/60	1.04[a]		1.60[a]	
(f)	30/70	1.07[a]	1.06 (71.5%)		2.343 (28.5%)
(g)	0/100		0.082 (50.0%)		7.84 (50.0%)
Cured phenolic/PEO ratio					
(a)	100/0	3.24			
(b)	80/20	3.18			
(c)	60/40	2.23		2.33	
(d)	50/50	1.80		1.41	
(e)	40/60	1.47[a]	0.93 (50.0%)		1.64 (50.0%)
(f)	30/70	1.39[a]	0.44 (37.6%)		2.35 (63.4%)

[a] This signal noise ratio is insufficient for reliable bi-exponential analysis.

inter-polymer associations is formed at the expanse of the PEO crystallinity and complete homogenous, amorphous, blend is established when the phenolic content reaches higher than 40 wt.%.

3.4. T_1^H relaxation time

The T_1^H relates the motion averaged over larger domain, and thus reveal slight different motional behavior than that from the $T_{1\rho}^{H}$. The drastic change of the molecular dynamics with composition in the phenolic/PEO blend clearly illustrated the T_1^H distributions for the uncured (Fig. 7) and the cured phenolic/PEO blends (Fig. 8). The locations and the width parameters for both samples are summarized in Table 4 for comparison. Absence of the multiple relaxation modes and narrow T_1^H distributions suggested that, apart from pure phenolic, the structure and dynamics are highly uniform. Notice that as T_1^H is the average over few hundred Å scale and it is unlikely to have PEO crystallite larger than that size, the relaxation result is the average of the mobility from both the amorphous domain as well as the damping of motion caused by the PEO crystallites. This phenolic shows a relatively high T_1^H, (434.4 ms) as compared to that of the neat PEO (189.1 ms) which also indicated the more rigid framework for phenolic, similar to that from $T_{1\rho}^{H}$. Interestingly, T_1^H relaxation of the blend deviates from a simple weight sum average from the two parent components and shows a minimum (22.6 ms) at 40/60 (phenolic/PEO) which indicated that the blend has the highest overall mobility. In fact, this sample appears to be gel like simply by visual examination. Based upon prior IR study, non-bonded hydroxyl group is completely absent at this composition [24]. A simple calculation with complete pairing of the hydrogen bonding shows approximately four ethylene oxide units that surround every hydroxyl group in the phenolic. The hypothetical structure is depicted in Fig. 9.

When PEO increases beyond 60 wt.%, insufficient hydroxyl is available to hydrogen bonding with PEO,

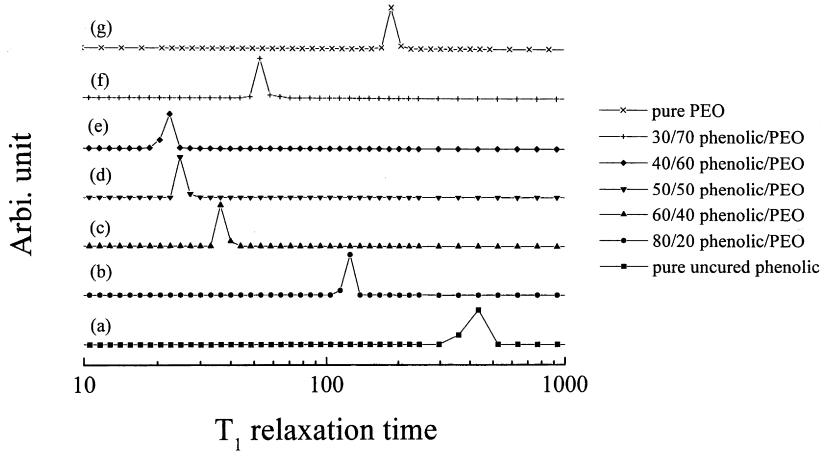

Fig. 7. The T_1^H relaxation time distribution of PEO, uncured phenolic, and their blends at 40°C. (a) 100/0 (■); (b) 80/20 (●); (c) 60/40 (▲); (d) 50/50 (▼); (e) 40/60 (◆ (f) 30/70 (+); (g) 0/100 (×), phenolic/PEO blends.

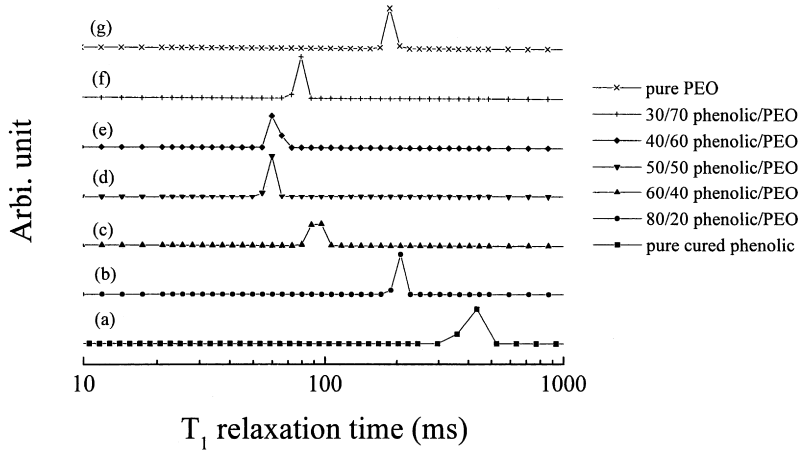

Fig. 8. The T_1^H relaxation time distribution of PEO, cured phenolic, and their blends at 40°C. (a) 100/0 (■); (b) 80/20 (●); (c) 60/40 (▲); (d) 50/50 (▼); (e) 40/60 (◆); (f) 30/70 (+); (g) 0/100 (×), phenolic/PEO blends.

more crystalline PEO appears. The crystalline PEO, which homogeneously immersed in the amorphous domain (phenolic/amorphous PEO), leads to the decrease of the over-all phenolic/PEO mobility and results in the gradual increase of T_1^H with increasing PEO. In the PEO rich regime, crystalline PEO has damped the motion averaged over longer scale, although within shorter scale the phenolic segmental motion is found to increase towards that of the pure amorphous PEO. In contrast, too much phenolic in the phenolic rich regime has reduced the over all motion. The balance of these two factors lead to an optimum mobility (shortest T_1^H) occurs at the 40/60 (phenolic/PEO) composition.

Table 4
The location and the width parameters of the T_1^H relaxation dispersion of PEO, and uncured, cured phenolic and their blends at 313.15 K, respectively

	T_1 (ms)[a]	Full width half maximum[b] [log(ms)]
Uncured phenolic/PEO ratio		
100/0	434.37	0.131
80/20	125.83	0.057
60/40	36.45	0.055
50/50	24.90	0.050
40/60	22.64	0.060
30/70	53.37	0.051
0/100	189.07	0.050
Cured phenolic/PEO ratio		
100/0	425.21	0.131
80/20	207.98	0.056
60/40	97.03	0.062
50/50	60.25	0.048
40/60	60.25	0.062
30/70	80.19	0.055
0/100	189.07	0.050

[a] The center of mass of T_1 distribution.
[b] Taken as the full width at half height in the log normal scale.

Similar reduction in T_1^H (and an increase of motion relative to pure component) are also observed for blends after curing, however they are slightly higher than that of the uncured series with the same composition. The relaxation time elevation, and thus reduction in the mobility with curing is possibly associated with cross-linking which forms more restricted framework hindering molecular segmental motion. The lack of multiple relaxation modes and the narrow distribution, similar to that observed in the uncured case suggest that the system maintains high homogeneity and good miscibility regardless of the cross-linking [15].

Notice that $T_{1\rho}^H$ measurement suggest amorphous domain (composed of phenolic and amorphous PEO which are highly miscible) continue to increase in mobility with increasing PEO content (Table 3), while T_1^H suggests the overall motion is first decreased followed by an increase with increasing PEO. The discrepancy is merely a reflection of the ensemble average of motions occurring within different length scale detected by the two relaxation methods. In addition, the increase of segmental motion comparing to the parent blend components revealed by the $T_{1\rho}^H$ and T_1^H appears contradicting with T_g elevation and free volume reduction, as tight hydrogen bonding network is expected

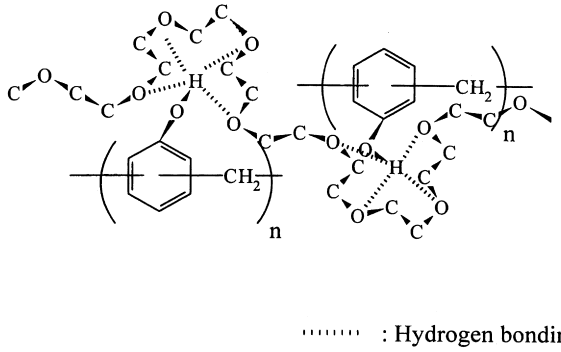

Fig. 9. Proposed conformation of hydrogen bonding schemes for 40/60 phenolic/PEO blend composition.

to restrict the framework mobility. Combining the fact that dense hydrogen bonding has created more amorphous PEO intimately mixed with phenolic and the fact that modifier PEO contains highly flexible ether group, the total molecular frame work mobility can actually be raised instead of been quenched. Owing to the difference of the scale involved in the ensemble average, the thermodynamic quantities, T_g and free volume are really not indicative of spin relaxation or the segmental motion. High mobility is still possible with reduced volume.

It is now clear that the inter-polymer hydrogen bonding network not only motivates the miscibility, reduced PEO crystallinity also improves the over all blend mobility. Relating to the dramatic increase in mobility, a substantial improvements in Izod impact strength upon blending with PEO is expected and indeed observed [25]. Changes in processibilities can also be expected, in spite of the T_g elevation. It would be of great interest to verify whether the mechanical properties are better correlated with the shorter scale motions revealed by $T_{1\rho}^H$ or with the larger domain average, including the crystalline PEO by T_1^H. Further, substantially enhanced segmental mobility beyond that of the pure PEO or phenolic, allows the phenolic/PEO blend to be used as polyelectrolyte, which is currently being explored [26].

4. Conclusion

Phenolic modified by PEO shows a positive T_g deviation and excess volume reduction due to formation of strong inter-molecular hydrogen bonding. However, mobility of phenolic/PEO blend is found to increase substantially, based upon both T_1^H and $T_{1\rho}^H$ measurements. Blending with phenolic has destroyed PEO crystallinity due to strong hydrogen bonding formation and the presence of more amorphous PEO raised the overall blend mobility. The blend with 50/50∽40/60 (phenolic/PEO) composition, which appears to be gel-like, give rise to highest mobility (the shortest T_1^H values). Compared to superb mobility of this blends, too much phenolic reduces the motion in phenolic rich region, while high PEO crystallinity in the PEO rich region also damped the overall molecular motion. The optimized behavior is attributed to the balance of total reduction of PEO crystallinity with the minimum amount of phenolic. Curing, which induces cross-linking has reduced the blend mobility. Nevertheless, the over-all motion is still higher than the parent components.

The study has also raised the issue that the blend physical properties cannot be judged solely from the structural heterogeneity, crystallinity, T_g, and free volume alone, but the over all molecular mobility should also be taken into consideration. The missing link can be easily bridged with proton relaxation time ($T_{1\rho}^H$ and T_1^H) methodologies which provide direct information regarding domain heterogeneity and molecular motion. In the case of phenolic/PEO, the apparent contradiction between the thermodynamics and the relaxation measurements is simply a reflection of the fact that thermodynamic and relaxation time measurements are ensemble average of different length scales. Although they are complementary to full understanding of blends, correlation between them should be exercised with caution.

Acknowledgements

Financial support of this research is provided by National Science Council, Taiwan, Republic of China, under the contract no. NSC-86-2113-N-008-004.

References

[1] Knop A, Pilot A. Phenolic resin. Berlin: Springer, 1985.
[2] Wu HD, Ma CCM, Lee MS, Wu YD. Die Angew Makromol Chemie 1996;235:35–45.
[3] Wu HD, Ma CCM, Lee MS, Wu YD. J Appl Polym Sci 1996;62(1):227.
[4] Wu HD, Ma CCM. J Appl Polym Sci 1997;63:911.
[5] Zhang X, Solomon DH. Macromolecules 1994;27:4919–4926.
[6] Wu HD, Chu PP, Ma CCM. Polymer 1997;38(21):5419.
[7] Wu HD, Chu PP, Lee CT, Jen HT, Ma CCM. Polymer 1998;39(13):2859.
[8] Yang TP, Pearce EM, Kwei TK, Yang LN. Macromolecules 1987;22:1813.
[9] Coleman MM, Serman CJ, Painter PC. Macromolecules 1987;20:226.
[10] Kim HI, Pearce EM, Kwei TK. Macromolecules 1989;22:3374.
[11] Penning JP, John MRS. Macromolecules 1996;29:77.
[12] Stotele JJ, Soldi V, Pires ATN. Polymer 1997;38:1179.
[13] Wu HD, Ma CCM, Li MS, Su YF, Wu YD. J Composites, Part A: Appl Sci Manuf 1997;28A:895.
[14] Chu PP, Howard JJ. Macromol Symp 1994;86:229.
[15] Chu PP, Wu HD. Macromol Symp 1994;86:229.
[16] Wu HD, Lee CT, Ma CC. SAMPE, Tech Conf, No 29, 28 October 1997, Orlando, Florida, USA. p. 653.
[17] Fox TG. J Appl Bull American Phy Soc 1956;1:123.
[18] Sanchez IC, Lacombe RH. J Phys Chem 1976;80:2352.
[19] Lacombe RH, Sanchez IC. J Phys Chem 1976;80:2568.
[20] Takahashi Y, Tadokoro H. Macromolecules 1973;6:672.
[21] Kurosu H, Ando I. J Mol Struct 1990;239:149.
[22] Schilling FC, Tonelli AE, Cholli AL. J Polym Sci Polym Phys Ed 1992;30:91.
[23] Zhang X, Takegoshi K, Hikichi K. Macromolecules 1992;25:2336.
[24] Chu PP, Liu SH, Liu HW. Polymer Preprints 1997;38(1):880.
[25] Chu PP, Wu HD, Lee JC. J Polym Sci, Part B Polym Phys 1998;30(10):1647.
[26] Chu PP, Jen HP. Macromolecules 1999.